

Synthesis of magneto-responsive microswimmers for biomedical applications

Cite as: AIP Advances 11, 025312 (2021); doi: 10.1063/9.0000103

Presented: 2 November 2020 • Submitted: 21 October 2020 •

Accepted: 22 January 2021 • Published Online: 8 February 2021



View Online



Export Citation



CrossMark

Hayder A. Alshammari,¹  Nilay Gunduz Akdogan,² Pelin Erkoç,¹  and Ozan Akdogan^{1,a)} 

AFFILIATIONS

¹Engineering and Natural Sciences, Bahcesehir University, Istanbul 34353, Turkey

²Maritime Higher Vocational School, Piri Reis University, Istanbul 34940, Turkey

Note: This paper was presented at the 65th Annual Conference on Magnetism and Magnetic Materials.

^{a)}Author to whom correspondence should be addressed: ozan.akdogan@eng.bau.edu.tr

ABSTRACT

Interest in untethered mini and micro-robots has shown a significant increase lately, especially magneto-responsive swimmers. In this study, a soft sub-millimeter sized swimmer and a magnetic actuation system was developed. An extrusion-based 3D printer was used to form swimmers with three different types of magnetic content, Fe micro flakes and nanoparticles, and Nd-Fe-B micro flakes, were incorporated into polymeric binder material. Using milli- and micro-swimmers in biological environments demands the use of cyto-compatible materials that would disguise the magnetic materials from the immune system. In this study, particles were encapsulated in a gelatin-alginate-cellulose based hydrogel. Next, these microswimmers were steered along a path via the magnetic gradient created by a custom-made electromagnetic system. The base of the electromagnetic system was designed using a CAD computer program and three dimensionally (3D)-printed. Consisting of four independent solenoids, each two controlling the movement on an axis, the system was designed to move the microswimmers in a certain path. The solenoids were controlled by Arduino microcontroller board. The electrical current applied to the electromagnetic device in all the trials was 2 amperes, which generates a magnetic field in between 100 to 376 Gauss throughout the experiment area. Thus, a magnetic gradient from the center to the pole of the solenoid was established. The magnetic and chemical behavior of these materials were compared based on their magnetic responsiveness and 3d printability. Developed magneto-responsive microswimmers could be used in biomedical robotics and drug delivery applications.

© 2021 Author(s). All article content, except where otherwise noted, is licensed under a Creative Commons Attribution (CC BY) license (<http://creativecommons.org/licenses/by/4.0/>). <https://doi.org/10.1063/9.0000103>

I. INTRODUCTION

Microswimmers have been widely explored over the last decade as a miniaturized device for minimal medical interventions because of their immense ability for smooth operation in hard to reach areas of the human body.¹ Through recent advances, the functionality, strength, and flexibility of micro-swimmers have been improved as well as the versatility of energy sources.² Energy sources include acoustic-,^{3,4} photo-,⁵⁻⁷ and magnetic-actuation⁸⁻¹² are used to move and control these swimmers. Microswimmers with such features can be integrated into- and improve various areas in the biomedical sector such as tissue generation,¹³ precise drug delivery,¹⁴ cargo transportation,¹⁵ and micro-mixing.¹⁶

To achieve these tasks and adapt with the environment, different shapes and sizes were experimented such as helical,¹⁶

dolphin,¹⁷ sheet,⁹ screw,¹⁸ sperm-,¹⁹ jellyfish-,¹² and octopus-shaped²⁰ magnetic milli-^{9,21,22} and micro-swimmers.^{12,16,18,23} Magnetic fields are the most favorable means of actuating and controlling micro-swimmers due to their harmless interaction with biological entities, their adjustable range of operation, and the ability to manipulate the magnetic domains of the materials.^{24,25}

However, magnetic material based small scale swimmers would cause undesirable host responses,¹⁵ which demands the necessity for a biocompatible shield to disguise the swimmer from the immune system.²⁶ The micro-swimmers introduced in this study possess a combination of the magnetic and biocompatible features. In a study performed by this group, the toxicity of Fe/Fe₃O₄ core-shell nanoparticles was higher on A549 lung cancer-cells than on NIH3T3 mouse embryonic fibroblasts cell lines,²⁷ which gives nanoparticle-based magneto-responsive

micro-swimmers developed in this study an advantage in various medical areas.

In addition, another study of the group showed that; CaCl_2 is a better candidate as a crosslinking agent for hydrogel which consists of gelatin, plant-based cellulose, and alginate. In this study, a cell viability test was done on murine fibroblast (NIH3T3) cells. Hydrogels crosslinked by glutaraldehyde (chemical crosslinking) showed high count of dead cells, while CaCl_2 hydrogel (ionic crosslinked) showed the opposite.²⁸

With the guidance of the control system developed in this study, these microswimmers can move in certain magnetic field paths. Multiple composites of materials with different ratios have been studied to find the best candidate to be used in the aforementioned applications.

II. MATERIALS AND EXPERIMENTAL SECTION

A. Materials

FeCl_2 (98%), NaBH_4 (96%), PEG (polyethylene glycol, 10kDa), hexane (96%), alginate (from brown algae), plant-based cellulose (fibers), and CaCl_2 (anhydrous calcium chloride) were obtained from Sigma Aldrich (MO, USA). Gelatin type A (from porcine skin, bioreagent grade, MP Biomedicals).

B. Experimental section

The 3d printer that was used in this study is a Hyrel Engine SR, equipped with a heated bed and the possibility of a multiple printing-head configuration. This 3d printer enables the user high

level of control over the printed shape and printing parameters such as printing and printing-head travel speed. Synthesis of the micro-swimmers starts with the production of magnetic additives. Afterwards, hydrogel-based fluid is prepared, and magnetic additives were incorporated in it. 3d printer was used to eject magnetic material loaded swimmers dropwise to CaCl_2 bath for curing. Later on, swimmers were dried and their movement performance in DI water were tested with homemade electromagnetic setup. (Figure 1)

1. Synthesis of magnetic materials

Laterally micron-sized iron flakes with 100-200 nm thickness were synthesized by surfactant assisted planetary ball milling of an irregularly shaped 10-micron sized startup material. The ball milling process was carried out at a speed of 700 rpm and for a period of 4-24 hours in a 4-vial MTI Corporation SFM-1 planetary ball mill system using stainless steel balls and vanadium steel vial. To ensure a flake shape, hexane and oleic acid were used as a dispersant and a surfactant, respectively. A three-time ethanol washing process was carried out and the flakes were stored in hexane. The same ball milling technique was used for 2-8 hours to produce approximately 150 nm thick Nd-Fe-B flakes.²⁹ Through the chemical reduction of FeCl_2 , Fe/ Fe_3O_4 core-shell nanoparticles with an approximate size of 20 nm were synthesized. The chemical reduction setup consisted of two flasks, one which containing the iron salt (FeCl_2) and the other contains NaBH_4 as a reduction agent; both reactants were dissolved in deionized water. The reaction was carried out at 1.7 NaBH_4 : FeCl_2 molar ratio in a Y-junction tube before it falls into a collection beaker that contains the coating agent, PEG.³⁰

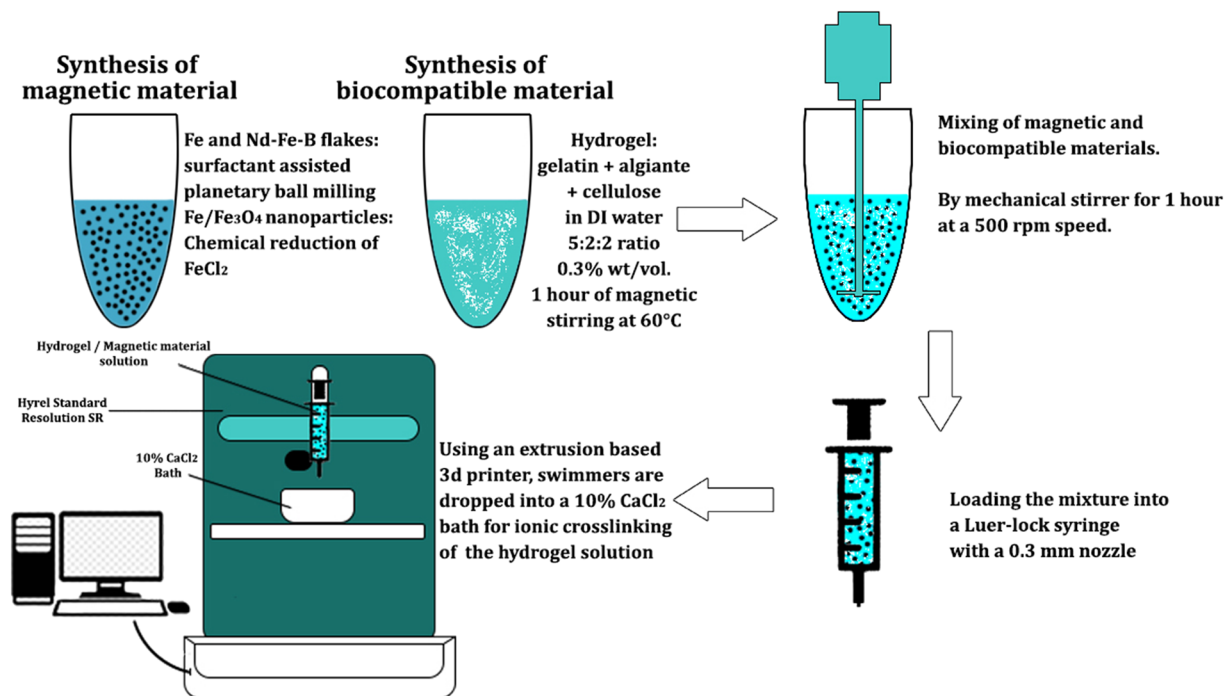


FIG. 1. Schematic of the synthesis procedure for the micro-swimmers.

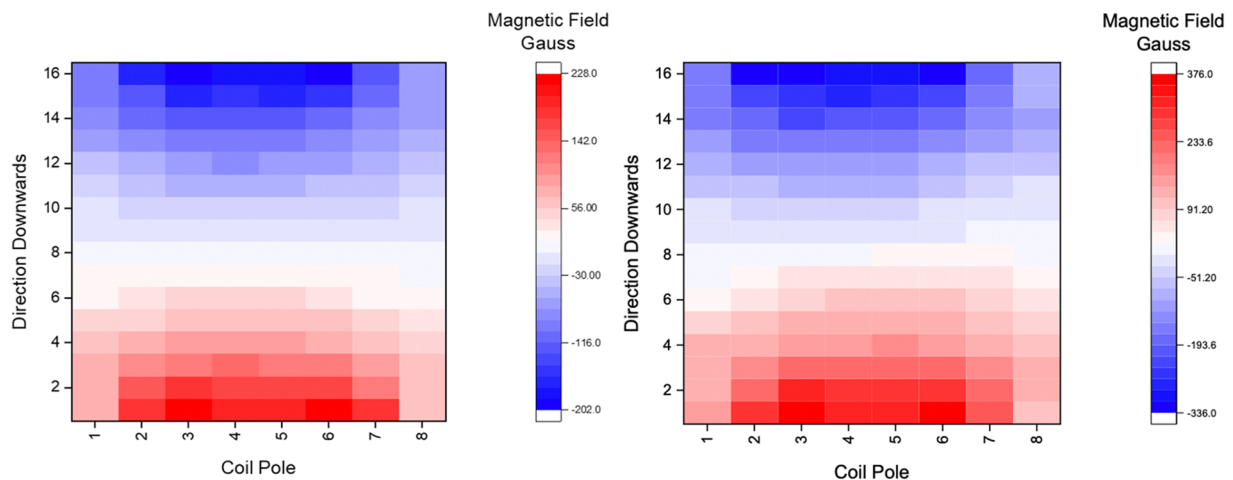


FIG. 2. Magnetic field gradient maps for 1 ampere (left) and 2 amperes (right) of applied electrical current.

2. Synthesis of magneto-responsive microswimmers

The hydrogel solution is made up of gelatin, alginate, and cellulose at a 5:2:2 weight ratio,²⁸ respectively, in deionized water with a 0.3% wt/vol. concentration and mixing them for 1 hour at 60°C using a magnetic stirrer. The solution was then mixed with the magnetic material for 1 hour using a mechanical stirrer. The mixture was deployed dropwise from an extrusion-based 3d printer, using a 0.3mm printing nozzle and a 1.47 mm³/s extrusion speed, into a CaCl₂ bath for crosslinking for 24 hours, then the swimmers were dried to achieve a micro scale.

3. Electromagnetic setup

Testing of the magneto-responsiveness of the microswimmers was done by using a four-direction electromagnetic coil system, controlled by an Arduino microcontroller and a four-channel relay module; this system is controlled manually by a digital interface coded by Processing software. The coils that make up the electromagnetic setup consist of 214 wraps of a 0.60 mm enamel coated copper wire, wrapped around a 3D printed frame with Fe-Co based steel core. (Detailed photo of the system could be found in [supplementary material Fig. 1](#)) Magnetic field mapping was done using a 1302 hallmark sensor; a map of the magnetic field gradient with the maximum magnetic field strength of 376 Gauss, are shown in [Figure 2](#).

III. RESULTS AND DISCUSSION

Room temperature hysteresis loops of the studied magnetic materials show a ferromagnetic behavior. While Fe flakes shows soft ferromagnetic response, Fe/Fe₃O₄ core-shell nanoparticles and NdFeB flakes shows hard ferromagnetic behavior with 350 Oe and 3.1 kOe coercivity, respectively ([Figure 3](#)).

Synthesis of the magneto-responsive microswimmers involves mixing the magnetic material with the biocompatible material solution in various concentrations and deploying them dropwise from

an extrusion-based 3D printer into the crosslinking medium. Synthesis trials showed that 0.5%, wt/vol. is the optimum concentration for the printability of the swimmers. Wet magneto-responsive swimmers have a body length of 1.5-3 mm, however, after drying them for 24 hours they shrink to a sub-millimeter size with diameter down to 207 μm ([Figure 4](#)). It has been found out that the size of the swimmers is only dependent on the printing parameters such as nozzle size and speed and not dependent on the magnetic additive type. Average size of the magnetic swimmers is 662.8 μm with a standard deviation (σ) of 112.7 μm. ([supplementary material Fig. 2](#)) It is also important to mention here that each 10 ml of the hydrogel/magnetic-additive solution produces approximately ~100 micro-swimmers.

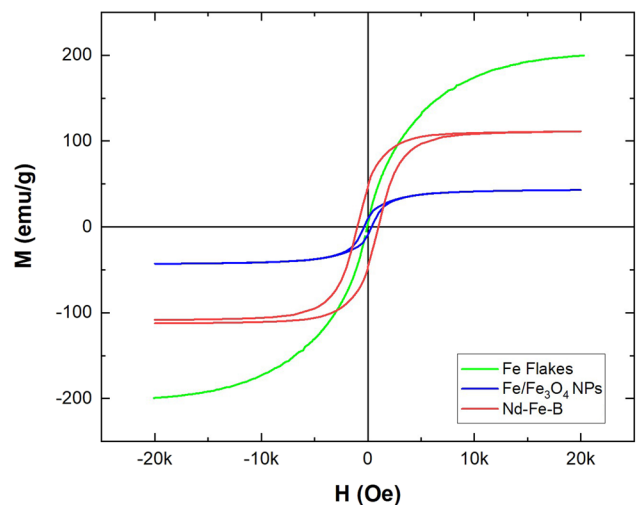


FIG. 3. Room temperature hysteresis loops of Fe flakes, Nd-Fe-B flakes, and Fe/Fe₃O₄ core-shell nanoparticles.

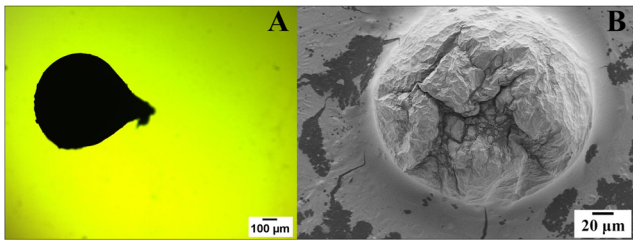


FIG. 4. (A) Light microscopy and (B) SEM image of Fe/Fe₃O₄ nanoparticles-based microswimmer.

Speed comparison between swimmers based on the magnetic material of choice with the same concentrations was done by observing the period that a swimmer takes to travel down the test area (Figure 5). The speeds were calculated by producing trajectory data of the videos taken from the movement of the swimmers. In order to produce the trajectory data; the manual tracking plugin in ImageJ software³¹ was used to export the position and direction dataset, which was then imported into the chemotaxis and migration software³² and plotted into the trajectory plot. (supplementary material Fig. 3) The comparison shows the different magneto-responsiveness of the microswimmers to the magnetic gradient created by the electromagnetic test setup.

Speed test of the swimmers showed that iron flakes-based microswimmers are faster than the other two types, which can be attributed to the difference in magnetic responsiveness of these magnetic materials with iron flakes being the most responsive. The combination of the magnetic responsiveness of Fe flakes and the high magnetic field values demonstrated higher swimming speeds than previous studies.^{33–37} To prove this hypothesis, theoretical expected values were calculated. Magnetic force on a particle inside a magnetic gradient is defined as:

$$F_m = \nabla(\mathbf{m} \cdot \mathbf{B}) \quad (1)$$

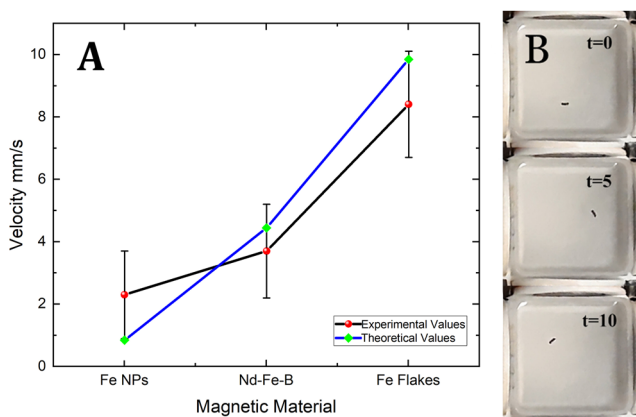


FIG. 5. (A) Speed comparison of magneto-responsive microswimmers based on the magnetic material (each measurement was repeated N=10 times); expected theoretical data is also included, (B) Snapshots from supplementary material, Supp.3 video of worm-shaped micro-swimmer (t=time in seconds).

where m and B represents the magnetic moment and the applied field, respectively. In the biological applications, nanoparticles will be deployed in certain fluids in which there will be a force that acts against these particles; the drag force or Stoke's Law:³⁸

$$F_d = 6\pi\eta Rv \quad (2)$$

Where η , R and v represents the fluid viscosity, the hydrodynamic radius of the particle, and the velocity of the particle, respectively.³⁹ Hydrodynamic radius and fluid viscosity values were taken as $331.4 \mu\text{m}$ and $8.9 \times 10^{-4} \text{ Pa}\cdot\text{s}$ (viscosity of DI water), respectively. Results of the calculations were included in Figure 5A. Theoretical and experimental data is comparable thus validating the results.

Demonstration videos in supplementary material, Supp.1 and Supp.2 show the movement and responses of Fe/Fe₃O₄ core-shell nanoparticle- and Fe flakes-based magneto-responsive microswimmers, respectively, in the test area with only the first being of the dry type. The video in Supp.3 shows a worm shaped microswimmer made up of three Fe/Fe₃O₄ NPs-based magneto-responsive microswimmers, responding to the magnetic field orders given by the digital interface.

IV. CONCLUSIONS

In this study, milli and micro-swimmers and electromagnetic setup were successfully developed to manually control the movement and direction of magneto-responsive swimmers using a custom-made computer software, which will expand the area of application of these swimmers. Substantial upgrades will be added to the setup in future studies to simulate different environments and obstacles. The biocompatibility of magneto-responsive microswimmers was improved by highly cytocompatible materials, which was previously proven through cell viability tests.²⁸ The results acquired from this study of highly responsive magnetic materials such as iron flakes, cytocompatible materials such as hydrogel, and a magnetic field control system with such magnetic field values, prove the potential of this combination to make a change in the medical industry.

SUPPLEMENTARY MATERIAL

See supplementary material for demonstration videos of the swimmers in the test setup. Supp.1 and Supp.2 show the movement of Fe/Fe₃O₄ core-shell nanoparticle- and Fe flakes-based swimmers, respectively. Supp.3 show the movement of a worm-shaped swimmer, made up of three Fe/Fe₃O₄ core-shell nanoparticle-based swimmers.

AUTHORS' CONTRIBUTIONS

All authors contributed equally to this work.

ACKNOWLEDGMENTS

This work was supported by BAP.2019-03.11 (Bahcesehir university).

DATA AVAILABILITY

The data that support the findings of this study are available within the article.

REFERENCES

- ¹B. J. Nelson, I. K. Kaliakatsos, and J. J. Abbott, "Microrobots for minimally invasive medicine," *Annu. Rev. Biomed. Eng.* **12**, 55–85 (2010).
- ²J. Li, B. de Ávila, W. Gao, L. Zhang, and J. Wang, "Micro/nanorobots for biomedicine: Delivery, surgery, sensing, and detoxification," *Sci. Robot.* **2**, eam6431 (2017).
- ³M. Kaynak *et al.*, "Acoustic actuation of bioinspired microswimmers," *Lab Chip* **17**, 395–400 (2017).
- ⁴H. O. Caldag and S. Yesilyurt, "Acoustic radiation forces on magnetically actuated helical swimmers," *Phys. Fluids* **32**, 092012 (2020).
- ⁵Q. Chen *et al.*, "Supracolloidal reaction kinetics of Janus spheres," *Science* **331**, 199–202 (2011).
- ⁶B. Qian, D. Montiel, A. Bregulla, F. Cichos, and H. Yang, "Harnessing thermal fluctuations for purposeful activities: The manipulation of single micro-swimmers by adaptive photon nudging," *Chem. Sci.* **4**, 1420–1429 (2013).
- ⁷M. Li, X. Wang, B. Dong, and M. Sitti, "In-air fast response and high speed jumping and rolling of a light-driven hydrogel actuator," *Nat. Commun.* **11**, 3988 (2020).
- ⁸S. Miyashita, S. Guitron, M. Ludersdorfer, C. R. Sung, and D. Rus, "An untethered miniature origami robot that self-folds, walks, swims, and degrades," in *Proceedings of IEEE International Conference on Robotics and Automation* (IEEE, 2015), pp. 1490–1496.
- ⁹E. Diller, J. Zhuang, G. Zhan Lum, M. R. Edwards, and M. Sitti, "Continuously distributed magnetization profile for millimeter-scale elastomeric undulatory swimming," *Appl. Phys. Lett.* **104**, 174101 (2014).
- ¹⁰A. Servant, F. Qiu, M. Mazza, K. Kostarelos, and B. J. Nelson, "Controlled in vivo swimming of a swarm of bacteria-like microrobotic flagella," *Adv. Mater.* **27**, 2981–2988 (2015).
- ¹¹R. W. Carlsen, M. R. Edwards, J. Zhuang, C. Pacoret, and M. Sitti, "Magnetic steering control of multi-cellular bio-hybrid microswimmers," *Lab Chip* **14**, 3850–3859 (2014).
- ¹²G. Z. Lum *et al.*, "Shape-programmable magnetic soft matter," *Proc. Natl. Acad. Sci. U. S. A.* **113**, E6007–E6015 (2016).
- ¹³M. T. Tolley *et al.*, "A resilient, untethered soft robot," *Soft Robot* **1**, 213–223 (2014).
- ¹⁴M. Sitti *et al.*, "Biomedical applications of untethered mobile milli/microrobots," *Proc. IEEE* **103**, 205–224 (2015).
- ¹⁵C. Peters, M. Hoop, S. Pané, B. J. Nelson, and C. Hierold, "Degradable magnetic composites for minimally invasive interventions: Device fabrication, targeted drug delivery, and cytotoxicity tests," *Adv. Mater.* **28**, 533–538 (2016).
- ¹⁶H. O. Caldag and S. Yesilyurt, "Acoustic radiation forces on magnetically actuated helical swimmers," *Phys. Fluids* **32**, 092012 (2020).
- ¹⁷C. Zhang *et al.*, "Modeling and analysis of bio-syncretic micro-swimmers for cardiomyocyte-based actuation," *Bioinspir. Biomim.* **11**, 056006 (2016).
- ¹⁸A. Servant, F. Qiu, M. Mazza, K. Kostarelos, and B. J. Nelson, "Controlled in vivo swimming of a swarm of bacteria-like microrobotic flagella," *Adv. Mater.* **27**, 2981–2988 (2015).
- ¹⁹I. S. M. I. Khalil *et al.*, "Sperm-shaped magnetic microrobots: Fabrication using electrospinning," *Modeling, and Characterization* (2016).
- ²⁰Y. Dai *et al.*, "Untethered octopus-inspired millirobot actuated by regular tetrahedron arranged magnetic field," *Adv. Intell. Syst.* **2**, 1900148 (2020).
- ²¹Y. Dai *et al.*, "Untethered octopus-inspired millirobot actuated by regular tetrahedron arranged magnetic field," *Adv. Intell. Syst.* **2**, 1900148 (2020).
- ²²U. Culha, S. O. Demir, S. Trimpe, and M. Sitti, "Learning of sub-optimal gait controllers for magnetic walking soft millirobots," in *Conference on Robotics: Science and Systems*, 2020.
- ²³I. S. M. Khalil *et al.*, "Sperm-shaped magnetic microrobots: Fabrication using electrospinning," *Modeling, and Characterization* (2016).
- ²⁴K. E. Peyer, L. Zhang, and B. J. Nelson, "Bio-inspired magnetic swimming microrobots for biomedical applications," *Nanoscale* **5**, 1259–1272 (2013).
- ²⁵Y. Alapan, A. C. Karacakol, S. N. Guzelhan, I. Isik, and M. Sitti, "Reprogrammable shape morphing of magnetic soft machines," *Sci. Adv.* **6**, eabc6414 (2020).
- ²⁶H. C. M. Sun, P. Liao, T. Wei, L. Zhang, and D. Sun, "Magnetically powered biodegradable microswimmers," *Micromachines* **11**, 404 (2020).
- ²⁷O. Akdogan, N. Akdogan, B. Domaç, and S. Alkhatib, "Effects of PEGylated Fe–Fe₃O₄ core-shell nanoparticles on NiH3T3 and A549 cell lines," *Heliyon* **6**, e03124 (2019).
- ²⁸P. Erkoç *et al.*, "3D printing of cyto-compatible gelatin-cellulose-alginate blend hydrogels," *Macromol. Biosci.* **20**, 2000106 (2020).
- ²⁹N. G. Akdogan and O. Akdogan, "Synthesis of Nd-Fe-B/Fe hybrid micromagnets," *AIP Adv.* **9**, 125139 (2019).
- ³⁰O. Akdogan, N. Akdogan, B. Domaç, and S. Alkhatib, "Effects of PEGylated Fe–Fe₃O₄ core-shell nanoparticles on NiH3T3 and A549 cell lines," *Heliyon* **6**, e03124 (2019).
- ³¹C. T. Rueden *et al.*, "ImageJ2: ImageJ for the next generation of scientific image data," *BMC Bioinformatics* **18**, 529 (2017).
- ³²G. Trapp, Chemotaxis and Migration Tool.
- ³³I. C. Yasa, H. Ceylan, U. Bozuyuk, A. M. Wild, and M. Sitti, "Elucidating the interaction dynamics between microswimmer body and immune system for medical microrobots," *Sci. Robot.* **5**, aaz3867 (2020).
- ³⁴H. Ceylan *et al.*, "3D-Printed biodegradable microswimmer for theranostic cargo delivery and release," *ACS Nano* **13**, 3353–3362 (2019).
- ³⁵B.-W. Park, J. Zhuang, O. Yasa, and M. Sitti, "Multifunctional bacteria-driven microswimmers for targeted active drug delivery," *ACS Nano* **11**, 8910–8923 (2017).
- ³⁶O. Yasa, P. Erkoç, Y. Alapan, and M. Sitti, "Microalga-Powered microswimmers toward active cargo delivery," *Adv. Mater.* **30**, e1804130 (2018).
- ³⁷U. Bozuyuk *et al.*, "Light-triggered drug release from 3D-printed magnetic chitosan microswimmers," *ACS Nano* **12**, 9617–9625 (2018).
- ³⁸Q. A. Pankhurst, J. Connolly, S. K. Jones, and J. Dobson, "Applications of magnetic nanoparticles in biomedicine," *J. Phys. D. Appl. Phys.* **36**, R167–R181 (2003).
- ³⁹Q. A. Pankhurst, J. Connolly, S. K. Jones, and J. Dobson, "Applications of magnetic nanoparticles in biomedicine," *J. Phys. D. Appl. Phys.* **36**, R167–R181 (2003).